Title
Evolution and chemical consequences of lightning-produced NOx observed in the North Atlantic upper troposphere

Journal
Journal of Geophysical Research Atmospheres, 105(D15)

ISSN
0148-0227

Authors
Crawford, J
Davis, D
Olson, J
et al.

Publication Date
2000-08-16

DOI
10.1029/2000JD900183

JOURNAL OF GEOPHYSICAL RESEARCH, VOL. 105, NO. D15, PAGES 19,795–19,809, AUGUST 16, 2000

Evolution and chemical consequences of lightning-produced NO_x observed in the North Atlantic upper troposphere

J. Crawford,[1] D. Davis,[2] J. Olson,[1] G. Chen,[2] S. Liu,[2] H. Fuelberg,[3] J. Hannan,[3] Y. Kondo,[4] B. Anderson,[1] G. Gregory,[1] G. Sachse,[1] R. Talbot,[5] A. Viggiano,[6] B. Heikes,[7] J. Snow,[7] H. Singh,[8] and D. Blake[9]

Abstract. Airborne observations of NO during the Subsonics Assessment Ozone and Nitrogen Oxides Experiment (SONEX) reveal episodes of high NO_x in the upper troposphere believed to be associated with lightning. Linkage to specific periods of lightning activity is possible through back trajectories and data from the National Lightning Detection Network. Lagrangian model calculations are used to explore the evolution of these high NO_x plumes over the 1-2 days between their introduction and subsequent sampling by NASA's DC-8 aircraft. Simulations include expected changes in HNO_3, H_2O_2, CH_3OOH, HO_2, and OH. Depending on the time of injection and dilution rate, initial NO_x concentrations are estimated to range from 1 to 7 ppbv. Similar to many previous studies, simulated HNO_3 concentrations tend to be greater than observations. Several possible explanations for this difference are explored. H_2O_2 observations are shown to be consistent with removal in convective activity. While it is possible that upper tropospheric CH_3OOH is enhanced by convection, simulations show such increases in CH_3OOH can be short-lived (e.g., < 12 hours) with no perceptible trace remaining at the time of sampling. High NO levels further prevent elevated levels of CH_3OOH from propagating into increases in H_2O_2. HO_2 is suppressed through reaction with NO in all cases. Simulated increases in OH exceeded a factor of 2 for some cases, but for the highest NO_x levels, loss of OH via $OH+NO_2$ offset production from HO_2+NO. Additional increases in OH of 30-60% could result from convection of CH_3OOH. A final point of discussion concerns how the chemistry within these plumes, their long-range transport, and their potential importance in sustaining background NO_x far from source regions present a challenge to global and regional model simulations.

1. Introduction

Our understanding of tropospheric photochemistry is critically dependent upon our understanding of the budget and distribution of NO_x ($NO+NO_2$). Through catalytic cycling in reaction with peroxy radicals, NO_x plays a dominant role in regulating the photochemical production of ozone [*Chameides and Walker*, 1973; *Crutzen*, 1973]. NO_x also influences the cycling of HO_x ($OH+HO_2$) [*Liu*, 1977; *Hameed et al.*, 1979]. One of the larger uncertainties that continues to demand attention is the role of lightning in the global NO_x budget. Current estimates for lightning NO_x allow for a source anywhere from 2 to 20 Tg N yr^{-1} with best estimates converging in the 2-6 Tg N yr^{-1} range [*Lawrence et al.*, 1995; *Levy et al.*, 1996; *Lee et al.*, 1997; *Price et al.*, 1997; *Bradshaw et al.*, 2000].

Data gathered from NASA's DC-8 during the Subsonics Assessment Ozone and Nitrogen Oxides Experiment (SONEX) [*Singh et al.*, 1999] show evidence for a substantial contribution from lightning to the NO_x budget over the North Atlantic during the fall of 1997 [*Liu et al.*, 1999; *Thompson et al.*, 1999; *Allen et al.*, 2000]. Furthermore, back trajectories in combination with data from the National Lightning Detection Network (NLDN) and long range (LR) lightning detection network have allowed for episodes of high NO measurements to be linked with specific periods of electrical activity far removed from the point of aircraft sampling [*Hannan et al.*, 2000]. This linkage allows for some exploration of the chemical evolution of this lightning-generated NO_x during transport.

This paper addresses the following issues: (1) observations of elevated NO_x during SONEX and evidence for a lightning origin followed by long-range transport, (2) Lagrangian calculations examining possible scenarios for the chemical evolution of such air masses during transport, and (3) implications these results have for understanding the global NO_x budget and efforts to simulate it.

[1]NASA Langley Research Center, Hampton, Virginia.
[2]School of Earth and Atmospheric Sciences, Georgia Institute of Technology, Atlanta.
[3]Department of Meteorology, Florida State University, Tallahassee
[4]Solar Terrestrial Environment Laboratory, Nagoya University, Toyokawa, Aichi, Japan.
[5]Institute for the Study of Earth, Oceans, and Space, University of New Hampshire, Durham.
[6]Air Force Research Laboratory, Hanscom Air Force Base, Massachusetts.
[7]Center for Atmospheric Chemistry Studies, University of Rhode Island, Narragansett.
[8]NASA Ames Research Center, Moffett Field, California
[9]Department of Chemistry, University of California, Irvine

Paper number 2000JD900183.
0148-0227/00/2000JD900183$09.00

2. Observations

The SONEX campaign consisted of 14 flights between October 13 and November 12, 1997. Flights focused on collecting data from the upper troposphere with more than 80% of data coming from altitudes above 6 km. NO_x levels encountered on three flights were substantially higher than those observed for other flights (see Figure 1). The flights on October 29 and November 3 and 9 disproportionately contributed to the total NO_x burden observed during the mission and suggest that the total NO_x burden is significantly influenced by highly localized plumes of NO_x. Average and median statistics given in Table 1 show that these three flights encountered NO levels more than 3 times greater than typically observed. Furthermore, the average NO for the total data set decreases by 40% when observations for these three flights are not included. The change in median NO is much smaller, signifying that a large portion of the total NO_x burden existed in concentrated plumes. Given the limited sampling of only 14 flights, the quantitative usefulness of the statistics in Table 1 may be questioned, and the importance of plumes to NO_x over the North Atlantic may also be viewed with some skepticism. Nevertheless, a large contribution for plumes to average NO_x over the eastern United States/North Atlantic has also been documented in the more extensive Nitrogen Oxides and Ozone Measurements along Air Routes (NOXAR) data set [*Brunner et al.*, 1998].

Evidence for a lightning origin for these NO_x plumes comes from several sources: back trajectories, NLDN and LR lightning data, and tracer correlations. The trajectories used here were provided by investigators from Florida State University [*Fuelberg et al.*, 2000]. Trajectories were calculated with a kinematic model using European Centre for Medium-Range Weather Forecasts (ECMWF) wind fields. The horizontal resolution was 1° with 31 vertical sigma levels. Temporal resolution for these data was 6 hours. More rigorous trajectory calculations were performed for the flight on October 29, which is highlighted in this work as well as by *Hannan et al.* [2000]. These trajectories were calculated with MM5 wind output using

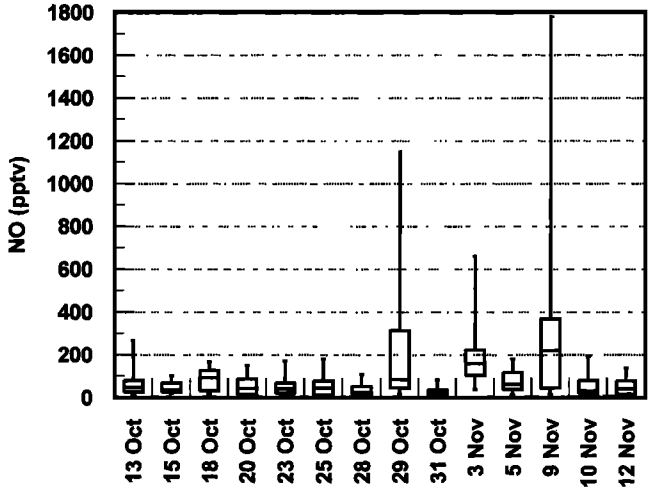

Figure 1. Distribution of NO observations for each flight during SONEX. The center line denotes the median value, boxes encompass the inner quartiles, and whiskers encompass the 5th and 95th percentiles. Data are filtered for altitude (6-12 km), daylight (solar zenith angle < 85°), and tropospheric air (O_3 < 120 ppbv).

Table 1. Average and Median NO for the Upper Troposphere During SONEX

Flights	Average NO	Median NO
Oct. 13-28; Nov. 5, 10, 12	62	42
Oct. 29; Nov. 3, 9	232	148
All flights	104	55

Altitude > 6 km, O_3 < 120 ppbv, and solar zenith angle < 85°

wind fields on grids of 30 and 90 km with 26 vertical sigma levels. The temporal resolution for October 29 was 1 hour. Figure 2 compares air mass origins based on back trajectories. In Figure 2a, flights without high NO_x episodes have trajectories showing a wide range of histories. In Figure 2b, however, flights encountering episodes of high NO_x reveal a trend involving air masses having passed over the Gulf of Mexico and Florida before turning north along the east coast of the United States. None of the trajectories in Figure 2a fit this trend, suggesting the Gulf of Mexico/Florida as the probable source region for the elevated NO_x.

NLDN data are useful in showing the coincidence between electrical activity and the trajectories in Figure 2b. The NLDN data represent a network of sensors detecting cloud-to-ground lightning flashes over the contiguous United States, and the LR data extend this capability over oceanic regions. More detailed information on these networks is given by *Cummins et al.* [1998] and *Idone et al.* [1998a,b]. Lightning activity during the SONEX time frame was frequently detected over the Gulf of Mexico and parts of the southern United States with some lightning observed over the Atlantic off the eastern coast of the United States as well. Only in the cases of the three flights having high NO_x did lightning activity coincide in time and location with trajectories. Specific details concerning the coincidence between trajectories and detected lightning flashes are provided in the case studies presented later.

Another indication of recent convection in the presence of lightning comes from the strong correlation between NO and ultrafine condensation nuclei (UFCN; > 4 nm diameter). Time series for NO and UFCN are shown in Figure 3. During each flight, elevated NO is accompanied by elevations in UFCN. Some exceptions occur for the first two NO events on November 3. The events in UFCN unaccompanied by elevated NO around 2100 UT on November 9 occurred in darkness but are associated with elevated NO_y. The correspondence between high NO and UFCN most likely results from new particle formation in recently convected air where existing particles have been removed by precipitation [*Wang et al.*, 2000]. For instance, on November 3 and 9, the correlations observed between NO and UFCN are not present for fine CN (> 15 nm diameter). On the other hand, fine CN data for October 29 correlate with NO just as well as UFCN data. This may relate to the time elapsed between sampling and injection of NO. As will be shown in the case studies, high NO sampled during flights on November 3 and 9 were most likely injected by lightning 18-24 hours prior to sampling; however, the high NO measured on October 29 appears to be at least 32 hours old. The longer processing time for the air sampled on October 29 may have allowed for not only new particle formation but significant particle growth as well. Episodes of high CN concentrations are not limited to these three flights; however, other encounters are most often attributed to aircraft influences [*Anderson et al.*, 1999].

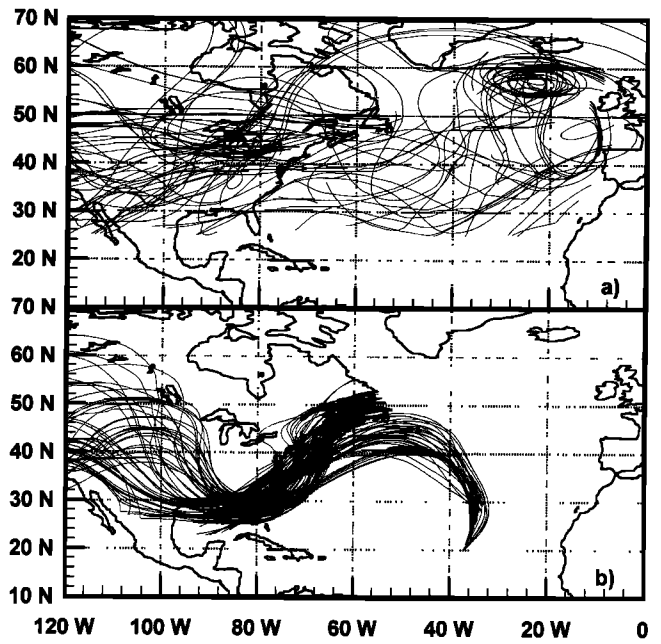

Figure 2. Kinematic back trajectories for air masses sampled during (a) all flights except October 29 and November 3 and 9 and (b) flights on October 29 and November 3 and 9.

In terms of other convective tracers, time series data reveal no clear correlations with NO. This lack of correlation, especially for tracers indicative of a polluted boundary layer, suggests that convective lifting of boundary layer NO does not contribute significantly to the part-per-billion levels of NO observed in these episodes. Some useful information can be also be gained from looking at tracer levels during convective periods relative to the rest of the data set. J. A. Snow et al. (A comparison of convective tracers during SONEX, submitted to *Journal of Geophysical Research*, 2000; hereinafter referred to as submitted manuscript, 2000) have provided an evaluation of convective tracers for the SONEX data set. Details concerning specific tracers as well as the conclusions of J. A. Snow et al. (submitted manuscript, 2000) regarding the high NO flights will be presented in the case studies.

3. Model Description and Approach

Lagrangian box model calculations can provide some insight on how these high NO_x plumes may have evolved between the introduction of fresh NO_x emissions and sampling by the DC-8 aircraft. The model used here is the same time-dependent photochemical box model described in earlier work [*Crawford et al.*, 1999, and references therein], the only modifications being that the location of the box can be changed in time and that calculations can be interrupted to adjust species concentrations, introduce flux terms, or introduce mixing parameters. The injection of NO by lightning can be simulated as an instantaneous increase in NO or as a continuous influx of NO over a specified period of time. The model is initialized with a "best guess" set of conditions at a point along the trajectory upstream of both the sampling point and the point of lightning influence. These initial conditions are brought to steady state before allowing the air parcel to travel along the trajectory. Once the parcel moves along the trajectory, events along the trajectory can be simulated with respect to injections and mixing.

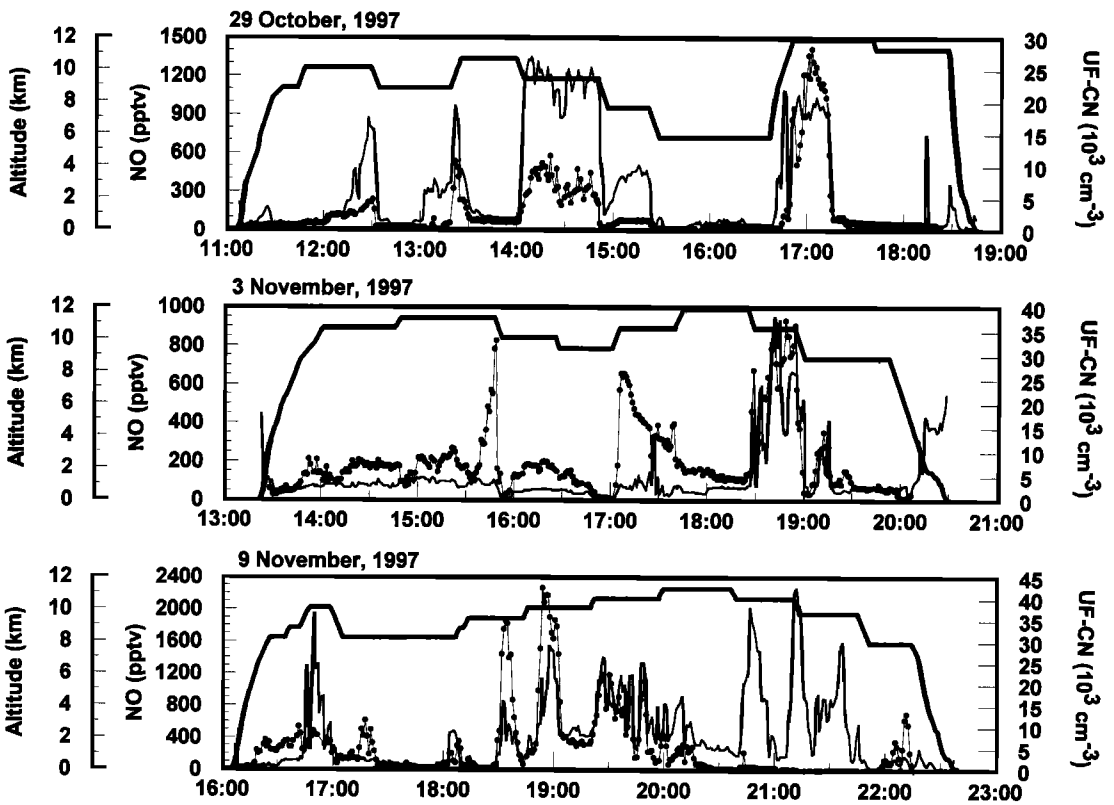

Figure 3. Time series of NO (dots), ultrafine CN (fine lines), and altitude (bold lines).

Table 2. Initial Conditions for Lagrangian Calculations of High NO Observed on October 29 (1700 UT), November 3 (1845 UT), and November 9 (1900 UT)

Parameter	1700, Oct. 29	1845, Nov. 3	1900, Nov. 9
Date	Oct. 27	Nov. 2	Nov. 8
Time, UT	1000	1345	1300
Latitude, °N	23.3	25.1	32.8
Longitude, °E	-90.6	-84.8	-86.5
Altitude, km	11.9	10.7	10.1
Temperature, °C	-60.2	-50.2	-49.1
Water vapor, ppmv	104	198	159
Ozone, ppbv	56	53	61
CO, ppbv	82	104	96
NO_x, pptv	50	50	50
Ethane, pptv	611	707	879
Propane, pptv	89	97	162
Benzene, pptv	8	22	13
Acetone, pptv	604	589	450
Methane, ppbv	1755	1767	1778
TOMS ozone, DU	260	276	290

When used for point calculations of airborne data, box models operate under the assumption of photochemical steady-state and constant ambient conditions. The Lagrangian reference frame requires different assumptions. Since the model is initialized upstream of the sampling point, assumptions must be made concerning the composition of the air parcel earlier in time. Assumptions must also be made about conditions along the trajectory such as perturbations to chemical species (e.g., NO_x from lightning and convective impacts on soluble and insoluble species), cloud conditions, and dilutive mixing. Specific assumptions used here are: 3-day dilution lifetime, clear-sky photolysis rates, and no change in basic chemical conditions during transport (e.g., O_3, CO, H_2O, temperature, pressure, etc. are the same as at the time of sampling by the aircraft).

The dilution lifetime was selected based on upwind NO_x concentrations necessary to match observations. As will be shown in the case studies, a 3-day dilution lifetime requires initial NO_x to be in the 1-4 ppbv range. This is in reasonable agreement with NO_x measurements in and around electrically active storms that have typically indicated a range of 0.5-5 ppbv [*Chameides et al.*, 1987; *Ridley et al.*, 1996; *Huntreiser et al.*, 1998, and references therein; *Brunner et al.*, 1998; *Höller et al.*, 1999; *Winterrath et al.*, 1999]. Some additional calculations based on no dilution and a dilution lifetime of 1.5 days will be presented to test the sensitivity of this assumption.

The assumption of clear-sky photolysis rates is adopted based on the altitude of the trajectories and observations (i.e., ~10 km). At this altitude, any attenuation of UV actinic flux from clouds above is unlikely and some enhancement from low-level cloudiness is quite probable. Furthermore, any thin cirrus generated by the convective outflow would most likely cause a local enhancement in photolysis rates. For these reasons, the use of clear-sky photolysis rates is believed to be a conservative estimate. The more difficult question concerning possible heterogeneous chemistry in the presence of cirrus clouds will be discussed in the interpretation of model results, but such chemistry is not incorporated into these model simulations.

4. Case Studies

Model calculations presented here are used to explore possible scenarios for the introduction and evolution of NO episodes from all three flights. Initial conditions for these calculations are given in Table 2. As noted earlier, the conditions in Table 2 are held constant in time with the exception of latitude, longitude, and Total Ozone Mapping Spectrometer (TOMS) total ozone. Trajectories for all three cases indicated rising air, although changes in altitude were small (~1 km for October 29/November 9 and ~2 km for November 3). These small changes are neglected, and calculations are fixed at the sampling altitude along the trajectory. The episode observed around 1700 UT on October 29, 1997 is investigated in greatest detail since it appears to represent the longest time and distance between injection and sampling for the episodes encountered.

These simulations examine the evolution of NO, NO_y, HNO_3, H_2O_2, CH_3OOH, HO_2, and OH for plumes from each flight. Table 3 also lists average measured values of HNO_3, H_2O_2, and CH_3OOH for comparison with simulated values. Two independent measurements of HNO_3 were available from the University of New Hampshire (aqueous scrub/ion chromatograph) and the Air Force Research Laboratory (chemical ionization mass spectrometer). Over the entire SONEX dataset, the agreement between these two techniques was considerably better than what might be inferred from the three cases presented in Table 3; thus neither estimate is preferred, but together they indicate the uncertainty in HNO_3 for each period. Although HO_x measurements were part of the DC-8 payload, a comparison is not pursued here since measurements were not available for two of the cases examined. *Brune et al.* [1999] also document unresolved discrepancies between modeled and measured HO_x for high NO as well as for solar zenith angles greater than 70°. One or both of these conditions occurred in each of the case studies.

4.1. Case 1: 1700 UT, October 29, 1997

On this flight the aircraft flew southward from the Azores to about 20°N and had several encounters with high NO levels of a few hundred pptv or more. The most prominent of these encounters occurred around 1700 UT with NO peaking near 1500 pptv and averaging about 1200 pptv (see Figure 3). J. A. Snow et al. (submitted manuscript, 2000) characterized this flight as being primarily influenced by marine convection. Although some influence from North American outflow was seen during the flight, it did not coincide with the event at 1700 UT. Data from Table 2 also show this encounter to be cleaner than those of later flights in terms of CO, CH_4, and nonmethane hydrocarbons (NMHCs).

The back trajectory for this high NO episode and its proximity to electrical activity is shown in Plate 1. The full trajectory, current position, and detected lightning flashes are depicted for four consecutive 6-hour periods. Plate 1 shows the air mass to be in the proximity of electrical activity almost

Table 3. Average Measured Values of HNO_3 and Peroxides During the Simulated NO_x Episodes

Species	1700 UT, October 29	1845 UT, November 3	1900 UT, November 9
HNO_3 (UNH)[a]	130 ± 26	55 ± 6	349 ± 32
HNO_3 (AFRL)[b]	239 ± 61	89 ± 31	223 ± 77
H_2O_2	50 ± 25	32 ± 10	32 ± 10
CH_3OOH	< 25	30 ± 9	35 ± 7

Values are given in pptv.
[a]University Of New Hampshire.
[b]Air Force Research Laboratory.

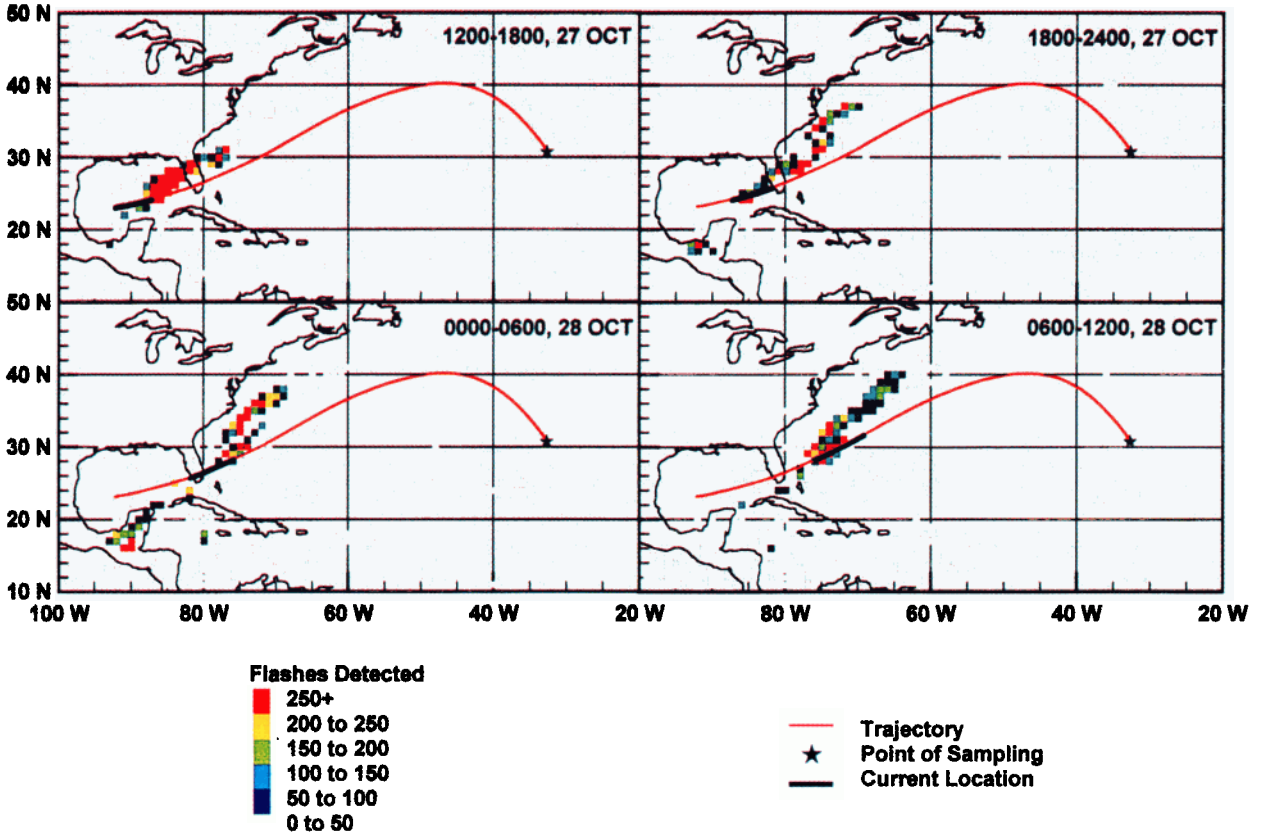

Plate 1. Proximity of lightning along the trajectory for the high NO sampled around 1700 UT on October 29, 1997. Bold line segments highlight the portion of the trajectory covered during each time period. Lightning data provided by NLDN and LR networks.

continuously for a 24 hour period; thus it is impossible to pinpoint a precise time and location when lightning NO_x may have been introduced into the air mass. In fact, it is quite possible that the sampled NO was introduced by multiple events over an extended time period.

Four different simulation scenarios have been executed for this high NO episode in order to examine sensitivities in the photochemistry to various assumptions. Details concerning these simulations are outlined in Table 4. The first scenario considers the perturbation and subsequent dilution of NO_x only. The second scenario builds upon the first by adding convective impacts on HNO_3 and peroxides. This includes the removal of HNO_3 and H_2O_2, the enhancement of CH_3OOH, and the subsequent dilution of these species with background concentrations. Background concentrations for HNO_3 (100 pptv), H_2O_2 (60 pptv), and CH_3OOH (25 pptv) used here are based on median upper tropospheric conditions observed during SONEX. The third and fourth scenarios examine the influence of assuming a 3-day dilution lifetime by repeating the second scenario with no dilution (scenario 3) and a dilution lifetime of 1.5 days (scenario 4).

Since the time and location for the introduction of lightning NO cannot be precisely determined, each scenario consists of three separate simulations: (A) early injection, (B) late injection,

Table 4. Lagrangian Calculation Scenarios for 1700 UT, October 29, 1997

Scenario	NO injection	Dilution Lifetime	HNO_3	H_2O_2	CH_3OOH
			(perturbed value/background value)		
1A	2500 pptv at -32 hours	3 day	no perturbation or dilution of HNO_3, H_2O_2 or CH_3OOH		
1B	3500 pptv at -50 hours	3 day	no perturbation or dilution of HNO_3, H_2O_2 or CH_3OOH		
1C	143 pptv hr^{-1} from -50 to -32 hours	3 day	no perturbation or dilution of HNO_3, H_2O_2 or CH_3OOH		
2A	2685 pptv at -32 hours	3 day	50/100	50/60	500/25
2B	3728 pptv at -50 hours	3 day	50/100	50/60	500/25
2C	168 pptv hr^{-1} from -50 to -32 hours	3 day	50/100	50/60	500/25
3A	1768 pptv at -32 hours	none	50/100	50/60	500/25
3B	1991 pptv at -50 hours	none	50/100	50/60	500/25
3C	110 pptv hr^{-1} from -50 to -32 hours	none	50/100	50/60	500/25
4A	4075 pptv at -32 hours	1.5 day	50/100	50/60	500/25
4B	6990 pptv at -50 hours	1.5 day	50/100	50/60	500/25
4C	252 pptv/hr from -50 to -32 hours	1.5 day	50/100	50/60	500/25

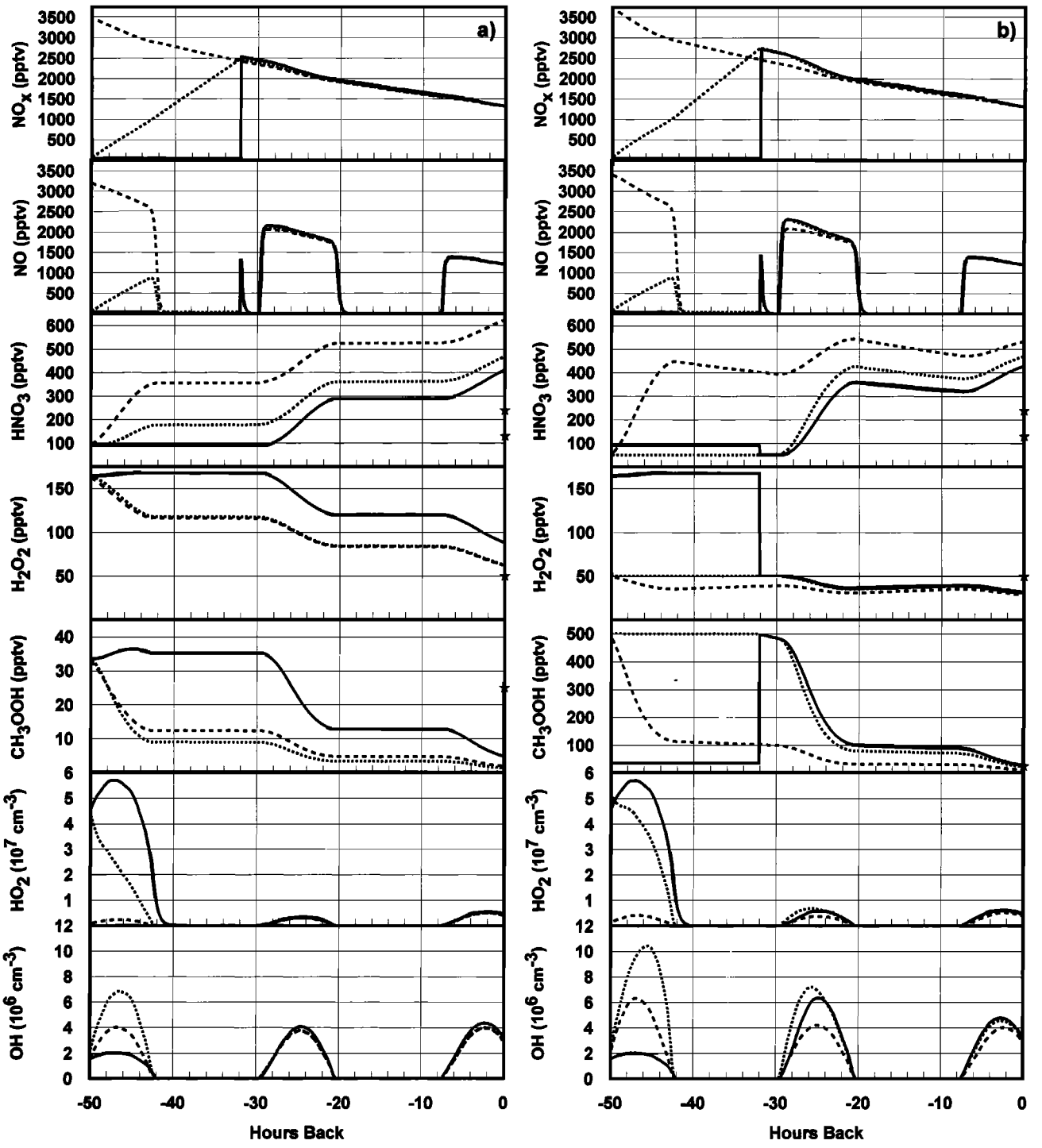

Figure 4. Time evolution for the Lagrangian calculation scenarios outlined in Table 4. Figure 4a shows scenario 1 (convective impact on NO only). Figure 4b shows scenario 2 (full convective impacts). Figure 4c shows scenario 3 (no dilution). Figure 4d shows scenario 4 (increased dilution). Each scenario shows results for late injection (solid line), early injection (dashed line), and continuous injection (dotted line). Stars on right-hand axis represent actual measured values given in Table 3.

and (C) continuous injection. The early and late injections involve an instantaneous injection of NO approximately 50 hours and 32 hours prior to being intercepted. Continuous injection assumes a continuous flux of NO for the 18-hour period between the times used for the early and late injections. In each case, the flux of NO was tuned to result in 1200 pptv of NO at the time of interception: 1700 UT on October 29, 1997.

Results for the different scenarios are shown in Figures 4a-d. The following discussion examines these results for each of the simulated species.

4.1.1. NO and NO_x. For all four scenarios, the time of NO injection has little impact on changes in NO and NO_x over the last 32 hours of these simulations; thus, the evolution of NO_x between the electrically active region and the point of

interception appears to be fairly robust despite no specific knowledge of when and how the NO_x was actually introduced.

The additional convective impacts of scenario 2 increase the oxidation rate of NO_x, thus requiring injected NO concentrations to be slightly greater than those for scenario 1. The enhanced oxidation is due mainly to the convective enhancement of CH_3OOH, which in turn produces higher OH values. The "no dilution" simulations (scenario 3), depicted in Figure 4c show substantially reduced NO injection levels, demonstrating that photochemistry plays a minor role in controlling the concentrations of NO and NO_x. The rapid dilution of scenario 4 requires NO injection levels of at least 4 ppbv and as much as 7 ppbv (Figure 4d). As noted earlier, this dilution rate appears to be a reasonable upper limit given that NO_x observations in and around electrically active storms have typically been in the 0.5-5 ppbv range.

Additional NO_x loss due to aerosol uptake of N_2O_5 and formation of peroxyacetylnitrate (PAN) was considered but found to be negligible. While an accurate assessment of aerosol surface area was not obtainable, a rough estimate of $10\mu m^2\ cm^{-3}$ was provided by B. Anderson (private communication, 1999) based on fine and ultrafine CN measurements. The uncertainty of this estimate must be regarded as high since numerous assumptions were necessary. Nevertheless, N_2O_5 levels averaged less than 10

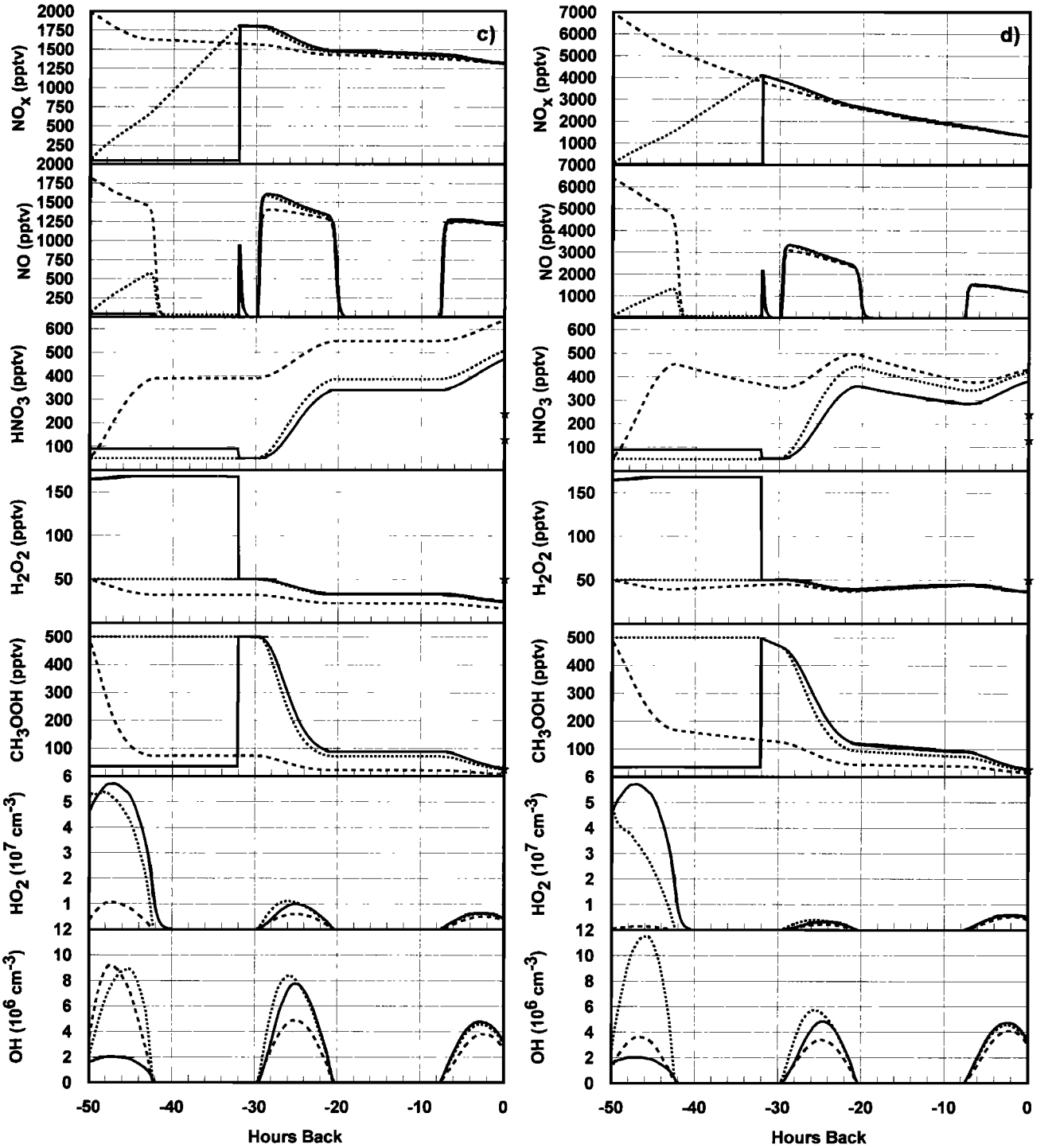

Figure 4. (continued)

pptv and had a 6-hour lifetime with respect to aerosol uptake; thus NO_x losses via this pathway were more than an order of magnitude slower than $OH+NO_2$. PAN formation was also negligible along the trajectory at less than 1 pptv.

4.1.2. HNO_3. For scenario 1, the increases in HNO_3 to levels between 400 and 600 pptv appear to rely primarily on the timing of the injection, with earlier injections leading to more HNO_3. These calculations exceed both HNO_3 observations by more than 100 pptv (see Table 3). This result is of concern, but it is not unusual in that overestimation of HNO_3 by models has been a common finding for studies of photochemistry in the remote upper troposphere [*Liu et al.*, 1992; *Schultz et al.*, 2000 and references therein].

When additional convective impacts are included (scenario 2), HNO_3 is initially lower due to the rainout perturbation and subsequent dilution, but HNO_3 increases more rapidly since NO_x oxidation is enhanced by the higher OH levels. Thus, final HNO_3 concentrations still exceed 400 pptv. The absence of dilution in scenario 3 (Figure 4c) shows photochemistry to be the primary driver for HNO_3, which displays behavior similar to the simulations in scenario 2. When doubling the dilution rate (scenario 4), predicted HNO_3 levels are still in the 400 pptv range; thus, predicted HNO_3 appears to be fairly insensitive to changes in either injection or dilution.

Although not shown in Figure 4, pernitric acid (HO_2NO_2) slightly decreases in these simulations from an initial value of ~30 pptv despite the increased NO_x. This is due to the decrease in HO_2, which more than offsets the increase in NO_2.

4.1.3. Peroxides. Scenario 1 (Figure 4a) shows elevated NO leading to decreases in both H_2O_2 and CH_3OOH. These decreases are closely related to the changes in HO_x. In this high NO_x environment, OH is elevated, and HO_2 is severely depressed. Radical cycling with NO dominates over peroxy radical self reactions that lead to peroxides, causing peroxide concentrations to steadily decrease. With the introduction of NO, production of H_2O_2 decreases from almost 70 pptv d^{-1} to about 2 pptv d^{-1}. Meanwhile, the photochemical lifetime of H_2O_2 due to photolysis and reaction with OH is slightly shorter due to greater OH (i.e., 2.3 days versus 2.5 days). Calculated H_2O_2 concentrations are slightly higher than the measured average of 50 pptv. The CH_3OOH budget undergoes a similar transformation with production falling from 30 pptv d^{-1} to about 1 pptv d^{-1}. The lifetime of CH_3OOH is also reduced from 1.1 days to 0.8 days. CH_3OOH calculations are consistent with the measurements showing values below the limit of detection (25 pptv).

Scenario 2 allows for convective impact on peroxides. In this scenario, the convective impact on H_2O_2 is assumed to be depletion through wet removal. Subsequent to convective depletion, changes in H_2O_2 are minimal, suggesting that the impact of convection is the most critical factor in determining the final H_2O_2 concentration. While the possibility exists that 500 pptv of CH_3OOH could have been transported to high altitude in conjunction with the lightning-induced NO_x, simulations show it to diminish so rapidly that any trace would be removed prior to sampling. In this scenario, the lifetime of CH_3OOH is even further reduced to 0.6 days. From this result, the limit-of-detection measurement for CH_3OOH (see Table 3) is not inconsistent with an earlier convective enhancement. The high NO_x concentration also prevents the decay of CH_3OOH from elevating H_2O_2; thus, the impact of the elevated peroxides is fleeting and otherwise unverifiable. The behavior of peroxides in this simulation differs from previous work showing elevations in CH_3OOH to propagate into H_2O_2 increases that persisted for a longer period [*Jaeglé et al.*, 1997; *Cohan et al.*, 1999; *Crawford et al.*, 1999]. In those simulations, NO_x levels were fairly low (e.g., less than 100 pptv). As with HNO_3, scenarios 3 and 4 show photochemistry to be the primary driver for peroxides as these quantities display behavior similar to the simulations in scenario 2.

Although not shown in Figure 4, the elevated levels of NO and CH_3OOH lead to increases in CH_2O. For instance, CH_2O in scenario 2 (initially in the 25-30 pptv range) increases to nearly 150 pptv, peaking about 6 hours after the convective event. Due to the elevated OH, however, CH_2O loss quickly takes over, reducing values to the 50-60 pptv range by the end of these simulations. This value is in reasonable agreement with the CH_2O measurement which indicates CH_2O to be at or below the 50 pptv detection limit. This final value might be higher if CH_2O was also transported from the boundary layer, but there is no convective perturbation to CH_2O in these simulations.

4.1.4. OH and HO_2. In each of these scenarios, the impact of NO is clearly shown to be suppression of HO_2 and enhancement of OH. For instance, scenario 1A (solid line, Figure 4a) shows peak HO_2 reduced by over an order of magnitude from almost 6×10^7 to less than 5×10^6 molecules cm^{-3} after the introduction of lightning NO_x at -32 hours. By contrast, OH doubles from 2×10^6 to 4×10^6 molecules/cm^{-3}. The enhancement of OH is further augmented by convective enhancement of CH_3OOH in scenario 2 which leads to integrated increases in OH of 30%, 28%, and 57% for simulations 2A-2C relative to 1A-1C. The larger increase for scenario 2C reflects the sustained enhancement of CH_3OOH at 500 pptv between -50 and -32 hours rather than the instantaneous enhancement of scenarios 2A and 2B. The lower NO_x levels of the "no dilution" simulation (scenario 3) allows for slightly higher HO_2, although it is still depressed by more than a factor of 5 following the introduction of lightning NO_x. OH is slightly higher due to the lower NO_x burden, but it is still quite similar to the values of scenario 2. HO_2 is suppressed most severely in scenario 4 which requires the highest NO_x concentrations, but the potential for increases in OH via $NO+HO_2$ are offset by the much greater burden of NO_x through NO_2+OH.

4.1.5. Uncertainties in calculated HNO_3. For all scenarios, calculated HNO_3 exceeded measured values by a significant amount. This discrepancy requires additional comment since it reflects a problem common to many previous studies of the upper tropospheric NO_x budget [*Liu et al.*, 1992; *Schultz et al.*, 2000, and references therein]. The SONEX data are no exception. Point calculations of upper tropospheric HNO_3 during SONEX exceed observations for more than 80% of the data with overestimations exceeding a factor of 2 for 60% of the data. One weakness of such point calculations is the assumption of photochemical equilibrium, which by definition assumes all NO_x to be secondary (i.e., recycled). Lagrangian calculations, however, do not assume photochemical steady-state. The dominance of fresh NO_x in the plume calculations presented here essentially eliminates the uncertainty regarding what fraction of sampled NO_x might be primary versus recycled. Nonetheless, several possible explanations for the overestimation of HNO_3 in these plume calculations remain. These include uncertainties in rate constants, uncertainties in convective impacts on HNO_3 and CH_3OOH, and possible heterogeneous removal of HNO_3 not included in these calculations.

The importance of accurate rate constants can be evaluated in light of recent studies of the rate constants for $OH+NO_2$ [*Dransfield et al.*, 1999] and $OH+HNO_3$ [*Brown et al.*, 1999]. Using these recommendations under the conditions being

simulated here, the rate constant for $OH+NO_2$ is decreased by 25% and the rate constant for $OH+HNO_3$ is increased by 70%. In calculations using these revised rate constants, HNO_3 decreased by 18% on average with no scenario decreasing by more than 23%. This relatively small change is a result of several factors. First, NO_x represents a significant OH sink in these calculations; therefore, the decrease in the NO_2+OH rate constant allows for higher OH concentrations. This higher OH concentration somewhat offsets the impact of reducing the rate constant for HNO_3 formation. For HNO_3+OH, changing this rate constant had a negligible impact on calculations of HNO_3 since photochemical formation of HNO_3 exceeded loss by an order of magnitude in these calculations. In an equilibrium calculation where formation and destruction of HNO_3 are equal, changing this rate constant would be expected to have a significant impact. The strong role of dilution in scenario 4 led to the lowest impact from changing these rate constants with decreases in HNO_3 being only 13-15%.

In terms of estimating convective impacts on HNO_3 and CH_3OOH, the most extreme case for reducing the predicted HNO_3 would involve 100% removal of HNO_3 during the convective period accompanied by no enhancement in CH_3OOH. When combined with the rate constant reductions noted above, this assumption reduces HNO_3 concentrations to the 200-250 pptv range for late and continuous injection of NO_x. HNO_3 for the early injection cases remain in the 300-350 pptv range.

The possibility that HNO_3 has been removed (or converted back into NO_x) through heterogeneous reaction on aerosol has been proposed by several groups [*Chatfield*, 1994; *Fan et al.*, 1994; *Jacob et al.*, 1996; *Hauglustaine et al.*, 1996; *Lary et al.*, 1997; *Iraci and Tolbert*, 1997], but the details remain speculative. When combined with the rate constant reductions noted above, the lifetime of HNO_3 with respect to loss on aerosol must be a little less than 2 days to achieve reductions of HNO_3 to the 200-250 pptv range. Given the estimated 10 $\mu m^2 cm^{-3}$ surface area, this requires an effective sticking coefficient of about 0.01. This rapid loss rate compares with the 1-day lifetime required by *Jacob et al.* [1996] to explain upper tropospheric HNO_3 data over the South Atlantic Basin. Applying this sticking coefficient in point calculations for the full SONEX data set does not improve the agreement between calculated and observed HNO_3. Instead of being overestimated, HNO_3 is underestimated by more than a factor of 2 for over 70% of the data.

While these calculations do not consider the fate of HNO_3, it is important to acknowledge the importance of knowing whether HNO_3 is being lost or recycled through heterogeneous chemistry. Here, the NO_x level is so much greater than the HNO_3 concentration that recycling has only a negligible effect on the outcome of the simulation. The long-term evolution of NO_x, however, would be greatly affected by whether or not HNO_3 is being recycled. Given the median surface area for the SONEX upper tropospheric data (~7 μm^2 cm^{-3}) and the assumed sticking coefficient of 0.01, the median lifetime for HNO_3 with respect to heterogeneous reaction would be about 2.5 days. If recycling was to take place at this rate, the residence time of NO_x in the upper troposphere would be controlled more by transport than by conversion to HNO_3. This would also reduce the magnitude of the source required to sustain observed upper tropospheric NO_x levels.

Another heterogeneous possibility would involve loss of HNO_3 to cirrus ice clouds created by the convective outflow. The appeal of this option is that it is peculiar to convectively impacted data and would not extend to the SONEX data as a whole. This possibility has been demonstrated in the lab [*Abbatt*, 1997; *Zondlo et al.*, 1997] and in field data [*Weinheimer et al.*, 1998] but has been challenged by other studies showing it to be unlikely on theoretical [*Tabazadeh et al.*, 1999] as well as observational grounds [*Meilinger et al.*, 1999; *Feigl et al.*, 1999]. More recent studies reporting evidence of photochemical NO_x production in snowpack ice for both the Arctic and Antarctic regions support the idea that ice crystals might play an important role in the budget of reactive nitrogen in the upper troposphere [*Honrath et al.*, 1999; *Davis et al.*, 1999; *Jones et al.*, 2000]. If indeed HNO_3 was lost to cirrus ice clouds, exposure for 6-8 hours after convection would delay the onset of HNO_3 buildup and reduce predicted HNO_3 by 150-250 pptv.

Unfortunately, there is no clear explanation for the discrepancy between calculated and measured HNO_3. The possibilities outlined above only serve to demonstrate that considerable uncertainty remains in modeled mechanisms and rates for HNO_3 formation and loss. Quite clearly, though, convective NO_x plumes represent an important setting for studying the evolution of HNO_3 in the upper troposphere.

4.2. Case 2: 1845 UT, November 3, 1997

This flight sampled air within the North Atlantic flight corridor over Newfoundland. The most prominent high NO episode for this flight occurred around 1845 UT with NO peaking over 900 pptv and averaging 720 pptv (see Figure 3). This flight was not addressed by J. A. Snow et al. (submitted manuscript, 2000), but CH_3I and $CHBr_3$ values exceeding upper quartile values for the SONEX data are consistent with their criteria signalling marine convection. CO levels for this flight were the highest observed during SONEX, indicating continental influence; however, increases in NMHCs were more modest.

Plate 2 shows the back trajectory for this high NO episode and its proximity to electrical activity. Again, the full trajectory, current position, and detected lightning flashes are depicted for four consecutive 6-hour periods. Here, the introduction of lightning NO_x appears to have occurred most likely during a period about 18-24 hours prior to sampling. Note, however, that while the trajectory falls behind the region of strongest lightning after 2400 UT on November 2, the plume remains in trailing regions of weaker lightning activity as it continues up the east coast of North America. GOES satellite imagery shows no evidence of cloudiness in this trailing region crossed by the plume.

Figure 5 shows results for NO_x injections at 18 and 24 hours assuming a 3-day dilution lifetime and convective impacts on HNO_3 and peroxides (i.e., scenario 2). Similar to the case for October 29, the results for November 3 do not appear to be overly sensitive to the precise time of injection. The sensitivity to injection time here is even less since any injection during the period of darkness from 8 to 20 hours prior to sampling would yield similar photochemical results.

HNO_3 is overpredicted for this episode by more than a factor of 2, but the absolute magnitude of the overprediction (i.e., 100-200 pptv) is similar to that for October 29. As already noted, several possibilities exist for trying to explain these differences; however, these data lack the information necessary for a definitive explanation. Peroxide behavior is also similar to the October 29 simulations. The measured H_2O_2 level appears to be consistent with convective removal followed by minimal changes in concentration. Results for CH_3OOH again show that a 500 pptv convective enhancement would be largely removed prior to sampling, but in this case, a small residual amount remains. A

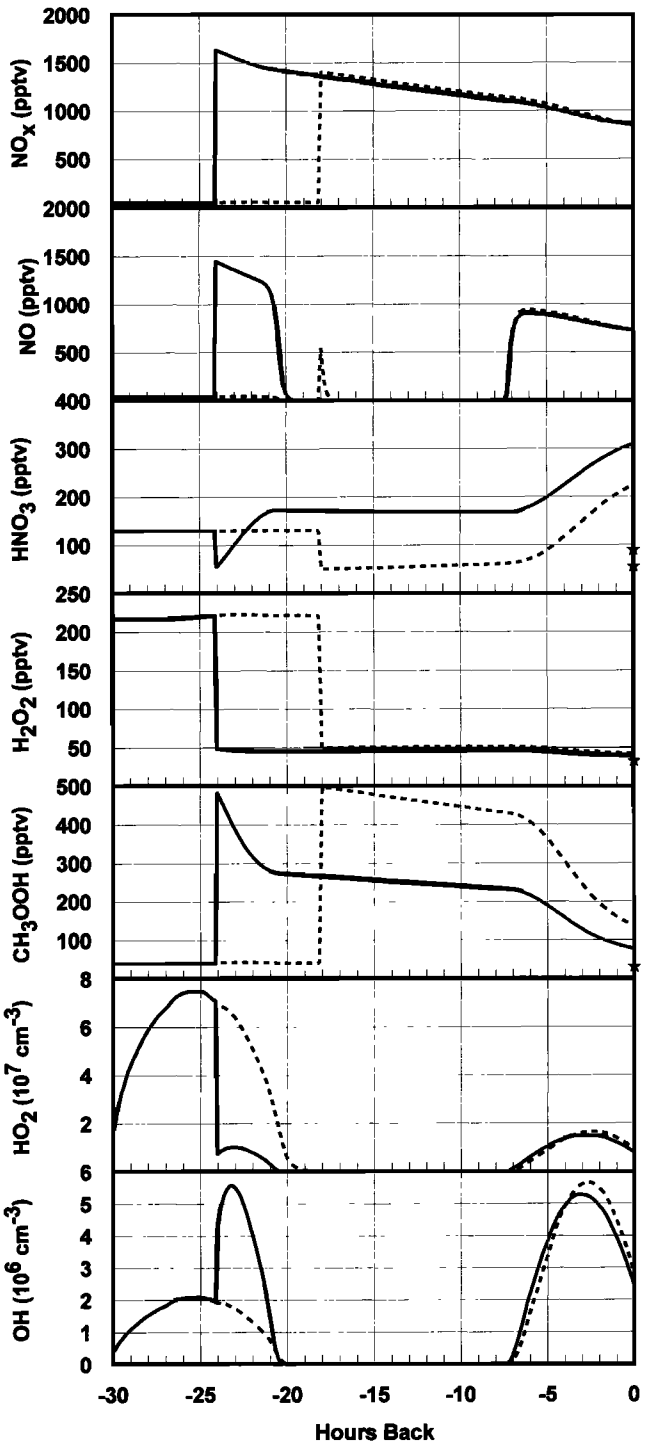

Figure 5. Lagrangian calculations for NO_x injections 18 hours (dotted lines) and 24 hours (solid lines) prior to 1845 UT on November 3, 1997. Dilution and convective impacts are the same as given for scenarios 2A-2C. Stars on right-hand axis represent actual measured values given in Table 3.

more reasonable upper limit for convective enhancement of CH_3OOH in this case would be around 400 pptv. Lastly, impacts on HO_x are similar to those for the October 29 case with HO_2 being suppressed while OH is almost 3 times greater.

4.3. Case 3: 1900 UT, November 9, 1997

The sampling region covered by this flight is essentially the same as observed during the flight on November 3. The NO levels encountered during this flight represent the highest concentrations observed during SONEX with levels peaking above 2000 pptv (see Figure 3). This flight was coordinated with the Swissair B-747 flying the automated NOXAR system which also encountered high NO (up to 3000 pptv) [*Jeker et al.*, 2000]. J. A. Snow et al. (submitted manuscript, 2000) noted evidence of both marine and continental convective signatures for this flight, suggesting that air was probably convected from the polluted marine boundary layer just off the east coast of North America. NMHCs were also substantially elevated with respect to the other high NO flights (see Table 2).

Plate 3 shows back trajectories for all three episodes of high NO and their proximity to electrical activity. All three cases show a similar history. Unlike the previous cases, here the air masses appear to have encountered lightning much further north. Again, the most likely period for NO_x injection appears to be about 18-24 hours prior to sampling, but trajectories show proximity to lightning over a substantially longer period. As with the case of November 3, these trajectories entered darkness 21 hours prior to sampling and entered daylight again 8 hours before sampling. Thus, the precise time that NO_x was injected is not critical to the photochemical results of these calculations. Calculations here focus on the second high NO episode peaking around 2300 pptv and averaging 1875 pptv.

Figure 6 shows results for NO_x injections at 18 and 24 hours assuming a 3-day dilution lifetime and convective impacts on HNO_3 and peroxides (i.e., scenario 2). This calculation is the first to show reasonable agreement with measured HNO_3; however, the 200-300 pptv of CH_3OOH remaining from the convective enhancement is in disagreement with the limit-of-detection measurement (25 pptv). One fundamental difference for this flight, however, is the latitude at which the convection was encountered. Unlike the previous cases, convective activity in the Gulf of Mexico region was absent, and the intersection between trajectories and strong electrical activity occurred further north by 5-10° latitude. Latitude distributions of CH_3OOH measurements from *O'Sullivan et al.* [1999] show that boundary layer mixing ratios could decrease by factors of 2 or more between 20° and 40°N. Thus convective enhancement of CH_3OOH would likely be diminished for convection occurring at higher latitudes.

Additional calculations show that reducing the convective enhancement of CH_3OOH to no more than 100 pptv would be more consistent with observations. This correction to CH_3OOH lowers estimates of HNO_3 to 210 and 160 pptv for injections at 24 and 18 hours, respectively. Since these values are within the uncertainty of the lesser of the HNO_3 measurements (see Table 3), it is tempting to accept the result as reasonable; however, to be consistent with the findings for the other two cases, it is necessary to comment on why this case does not overpredict HNO_3. Based only on surface area estimates, this plume (~19 $\mu m^2 cm^{-3}$) would have experienced more heterogeneous loss than the plumes of October 29 and November 3 (~10 μm^2 cm^{-3}). The distribution of particle sizes, however, indicates that the aerosol environment of November 9 may have been significantly different in composition. When only considering particles < 100 nm, the available surface area for November 9 was ~4 μm^2 cm^{-3} compared to ~10 μm^2 cm^{-3} for October 29 and 6 μm^2 cm^{-3} for November 3. If heterogeneous loss of HNO_3 was not important for the November 9 case, then the gas phase chemistry of this simulation may well be sufficient to explain observations. If heterogeneous chemistry did play a role, the agreement between the simulation and observations could indicate that the initial condition for HNO_3 in this simulation was too low. Based on

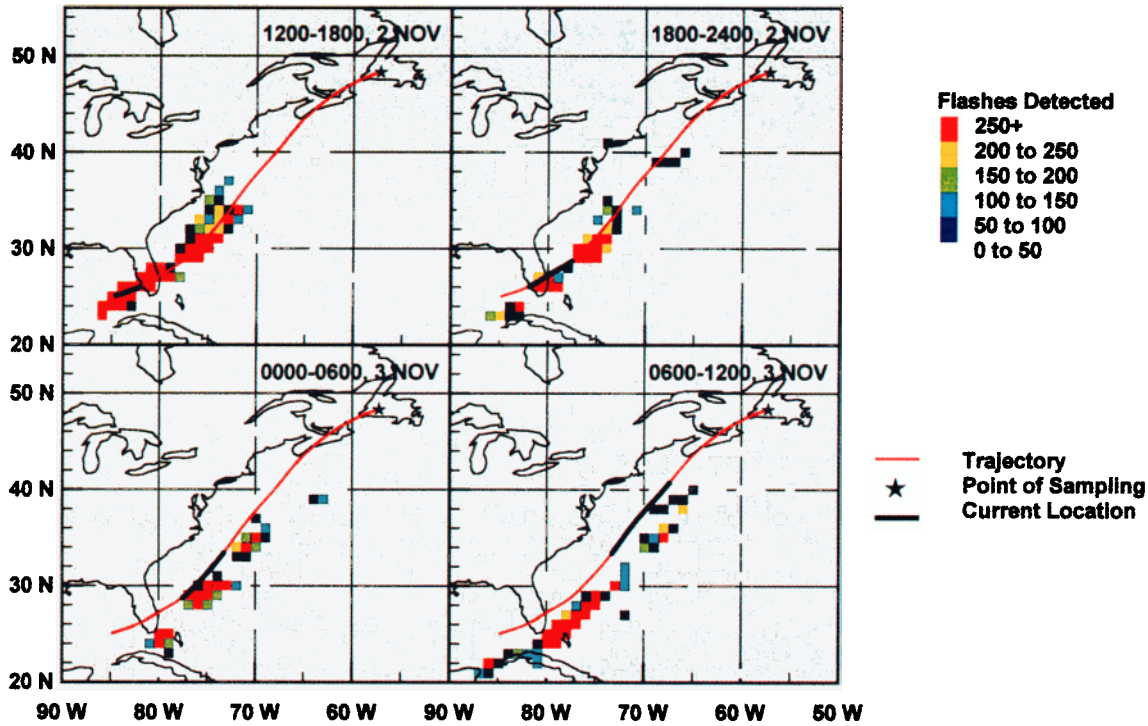

Plate 2. Proximity of lightning along the trajectory for the high NO sampled around 1845 UT on November 3, 1997. Bold line segments highlight the portion of the trajectory covered during each time period. Lightning data provided by NLDN and LR networks.

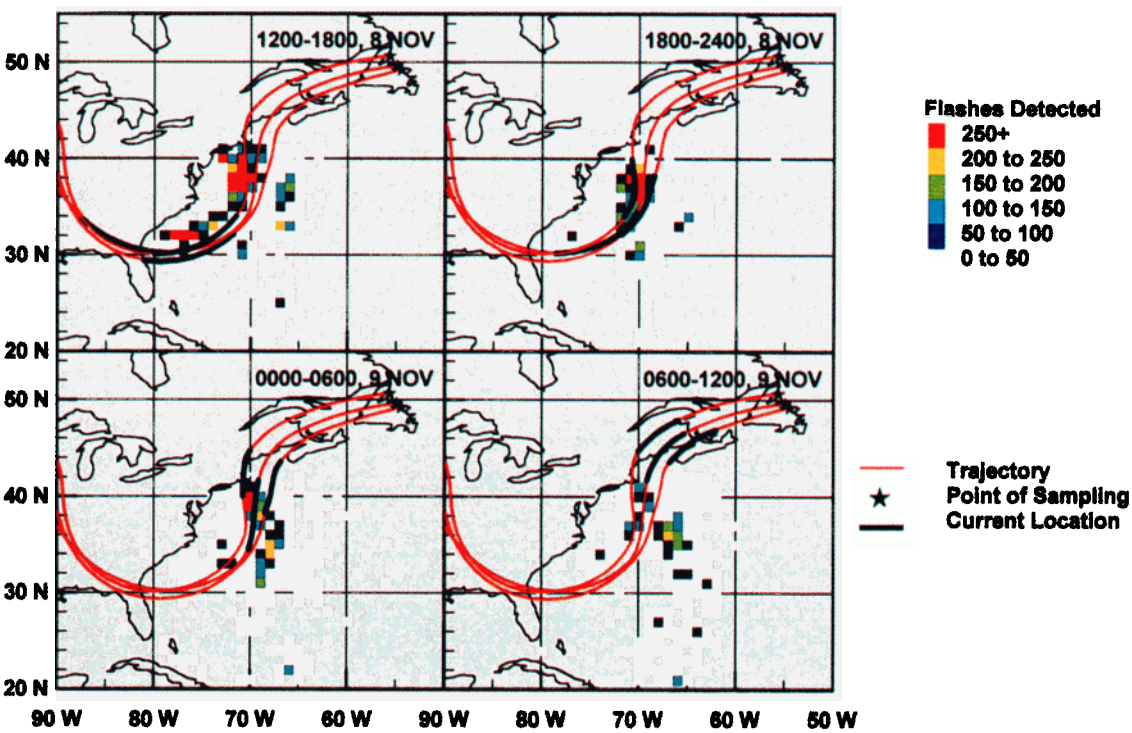

Plate 3. Proximity of lightning along the trajectory for the high NO sampled around 1900 UT on November 9, 1997. Bold line segments highlight the portion of the trajectory covered during each time period. Lightning data provided by NLDN and LR networks.

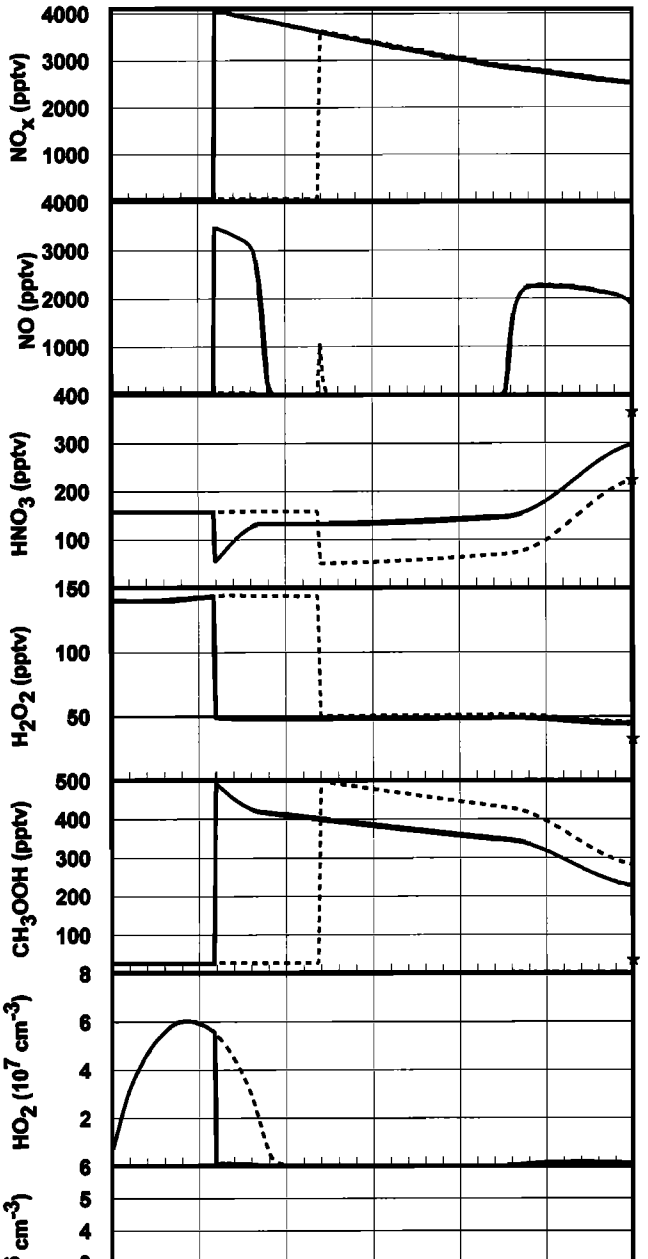

Figure 6. Lagrangian calculations for NO_x injections 18 hours (dotted lines) and 24 hours (solid lines) prior to 1900 UT on November 9, 1997. Dilution and convective impacts are the same as given for scenarios 2A-2C. Stars on right-hand axis represent actual measured values given in Table 3.

NMHC concentrations, the November 9 plume was the most polluted. This may indicate convection from a more polluted marine boundary layer just off the east coast of the United States. A second possibility is that the upper tropospheric portion of air mixed into the plume at the point of convection was impacted earlier by convection over the continental United States. Along with the NMHCs, such air would probably contain a significant amount of HNO_3 which would allow the plume to start with more than the 50 pptv assumed in these simulations.

Unlike HNO_3 and CH_3OOH, H_2O_2 exhibits behavior consistent with the other case studies. Again, the final concentration of H_2O_2 is consistent with wet removal during convection with only minor subsequent changes. HO_2 is more severely depressed than in the previous cases due to higher NO_x levels, but OH is essentially unchanged. Here, the gains in OH from HO_2+NO have been entirely offset by the loss of OH through OH+NO_2. Enhancements in OH should be expected to occur further downstream as NO_x levels become more diluted.

5. Implications of Plumes for Global Simulations

This study advocates that the NO_x distribution over the North Atlantic as suggested by SONEX data is likely to show strong signatures from lightning, although the nature of flight programs such as SONEX precludes any definitive statements. The detailed accounting of NO_x sources has been approached much more rigorously by other authors with respect to the SONEX data [*Liu et al.*, 1999; *Allen et al.*, 2000]. In spite of the difficulties of extrapolating field campaign programs to regional or global analyses, it is still useful to comment on the challenges of understanding the NO_x budget on these larger scales, many of which are highlighted by the SONEX data.

In recent years, the simulation of lightning NO_x in three-dimensional global and regional chemical transport models has been significantly improved by linking model convection with lightning [e.g., *Levy et al.*, 1996; *Flatøy and Hov*, 1997; *Houweling et al.*, 1998; *Penner et al.*, 1998; *Wang et al.*, 1998; *Stockwell et al.*, 1999]. These models typically correlate lightning with convective cloud top heights and use empirically based estimates for determining flash rates, cloud-to-ground versus intracloud fractions, vertical distribution of NO_x, and NO_x yield [e.g., *Liaw et al.*, 1990; *Proctor*, 1991; *Price and Rind*, 1992]. Given the benefits of increasingly detailed observations from satellites (e.g., optical transient detector and lightning imaging sensor) and the proliferation of ground networks such as the NLDN, further improvements in simulating the spatial and temporal distribution of NO_x from lightning are possible in the near future. Improved estimates for the vertical distribution of NO_x from lightning have also become available recently [*Pickering et al.*, 1998].

While simulation of lightning frequency and spatial distribution is expected to improve, chemical transport models have yet to deal with the plume aspect of lightning emissions. The importance of plumes relates to the highly nonlinear nature of O_3-HO_x-NO_x photochemistry which is particularly sensitive to NO_x concentration [*Liu et al.*, 1987]. A typical grid cell in a global model is on the order of 3°×5°; thus, averaging NO_x emissions from lightning over a grid cell can lead to substantial errors in their chemical impact. The need to resolve plume-scale chemistry rather than averaging over a grid cell has been addressed by modelers simulating the impact of highly local, industrial point emissions of NO_x within the urban boundary layer [*Sillman et al.*, 1990]. This problem has also been addressed more recently for aircraft emissions with treatment of plumes leading to reductions in model-predicted O_3 of 15-25% [*Meijer et al.*, 1997]. As an example, calculations of O_3 production for upper tropospheric conditions typical to SONEX were performed for the average NO values presented in Table 1. Calculations assuming the overall average NO (104 pptv) to be representative resulted in a daily net O_3 production rate 15%

greater than a weighted average of net O_3 production calculated separately for the three high NO flights (232 pptv) and the remaining flights (62 pptv NO).

Another important issue is the contribution of NO_x plumes in sustaining background NO_x. The SONEX data analyzed here suggest that plumes of high NO_x from lightning may remain relatively intact for at least several days allowing transport over distances of several thousand kilometers or more. Elevations in upper tropospheric NO_x far from source regions have also been noted in several other field studies [*Davis et al.*, 1996; *Jacob et al.*, 1996; *Crawford et al.*, 1997]. The impact of such long-range transport is absent from simulations that dilute lightning NO_x over a grid box at the moment of injection. By transporting concentrated plumes of NO_x over such distances before they fully dilute, the impact of lightning on background NO_x would be less localized with increased contributions to background NO_x at higher latitudes and other locations far from electrically active regions.

6. Summary

Episodes of high NO concentrations encountered during SONEX appear to have a lightning origin. Linkage to specific periods of lightning activity was possible through back trajectories and data from the National Lightning Detection Network. These episodes represent a small percentage of the total data set; however, they have a large impact on the average NO concentration. While the SONEX data set is too limited to quantify the importance of these NO_x plumes, average NO_x concentrations have also been shown to be sensitive to plume data in the much more extensive NOXAR data collected over the eastern United States and the North Atlantic [*Brunner et al.*, 1998].

Lagrangian calculations were used to explore the evolution of three of these high NO_x episodes. Several scenarios were simulated to cover the range of possible times for NO_x injection, various dilution rates, and convective perturbations to HNO_3 and peroxides. Depending on the time of injection and dilution rate, initial NO_x concentrations ranged from 1-7 ppbv. Values of 0.5-4 ppbv are supported by numerous field observations for NO_x in and around electrically active clouds.

Simulations of HNO_3 did not agree well with observations. For the October 29 case, expected HNO_3 concentrations of 400-600 pptv were fairly insensitive to initial conditions and exceeded observed values by 100 pptv or more. Factors possibly contributing to this overprediction included uncertainties in rate constants, convective impacts on HNO_3 and CH_3OOH, and heterogeneous chemistry. HNO_3 was overpredicted by more than factor of 2 for the November 3 case; however, the absolute difference between prediction and observations was similar to that of October 29. Prediction of HNO_3 on November 9 was within observed uncertainties; however, this agreement may have been fortuitous since the initial conditions for HNO_3 are more uncertain. Collectively, these Lagrangian calculations have proven to be useful in highlighting some of the difficulties in simulating HNO_3. While they have removed the uncertainty associated with assuming photochemical equilibrium, important questions still remain relating to the specifics of heterogeneous loss/recycling through exposure to aerosol or cirrus clouds as well as aerosol composition.

H_2O_2 simulations provided results consistent with convective removal for all three cases. Another factor contributing to the reduction of H_2O_2 was the high NO environment which effectively blocked further formation of H_2O_2 while leaving the loss of H_2O_2 unimpeded. The high NO environment impacted CH_3OOH similarly. While it is possible that CH_3OOH was convectively enhanced, simulations show perturbations to be short-lived with no perceptible trace remaining at the time of sampling. The November 9 case was an exception; however, the convection for this case was located further north where boundary layer concentrations of CH_3OOH might have been significantly less. While these calculations cannot verify the convective enhancement of CH_3OOH, it is not a trivial issue. For example, elevated CH_3OOH led to integrated increases in OH of 30-60% over the 50-hour simulations for the October 29 case.

The impact of lightning NO_x on HO_x has a strong dependence on the NO_x concentration. Suppression of HO_2 is common to all cases. This suppression of HO_2 through reaction with NO serves to elevate OH, but elevated NO_x levels also present an additional burden to OH through reaction with NO_2. Lightning NO_x for the October 29 and November 3 cases led to increases in OH by more than a factor of 2. On the other hand, the November 9 case illustrated conditions for which lightning NO_x caused no change in OH despite suppression of HO_2 by an order of magnitude. This condition would change further downstream as the NO_x continues to dilute and the competition between HO_2+NO and NO_2+OH begins to favor increased OH.

Finally, the SONEX data demonstrate the potential for plume-scale processes to be important in the chemistry and long-range transport of lightning NO_x. Both of these effects represent potentially significant uncertainties for regional and global chemical transport models.

Acknowledgments. We thank S Goodman and his team at NASA/Marshall Space Flight Center for providing access to data from the National Lightning Detection Network (Global Atmospherics Inc.) and Tom Kucsera of NASA/Goddard for his assistance in interpreting the data files. We also thank Reg Newell and Ken Pickering for helpful discussions of convective mixing

References

Abbatt, J P , Interaction of HNO_3 with water-ice surfaces at temperatures of the free troposphere, *Geophys. Res. Lett.*, *24*, 1479-1482, 1997

Allen, D. J., K. E. Pickering, G. Stenchikov, A. M. Thompson, and Y. Kondo, A three-dimensional total odd nitrogen (NO_y) simulation during SONEX using a stretched-grid chemical transport model, *J. Geophys. Res.*, *105*, 3851-3876, 2000.

Anderson, B. E., W R. Cofer, J. Crawford, G. L. Gregory, S. A. Vay, K. E. Brunke, Y. Kondo, M. Koike, H. Schlager, S. L. Baughcum, and E. Jensen, An assessment of aircraft as a source of particles to the upper troposphere, *Geophys. Res. Lett.*, *26*, 3069-3072, 1999.

Bradshaw, J. D., D. Davis, G. Grodzinsky, S. Smyth, R. Newell, S. Sandholm, and S. Liu, Observed distributions of nitrogen oxides in the remote free troposphere from the NASA Global Tropospheric Experiment programs, *Rev. Geophys.*, *38*, 61-116, 2000.

Brown, S. S., R. K. Talukdar, and A. R. Ravishankara, Reconsideration of the rate constant for the reaction of hydroxyl radicals with nitric acid, *J. Phys. Chem. A*, *103*, 3031-3037, 1999.

Brune, W. H. et al., OH and HO_2 chemistry in the North Atlantic free troposphere, *Geophys. Res. Lett.*, *26*, 3077-3080, 1999.

Brunner, D., J. Staehelin, and D. Jeker, Large-scale nitrogen oxide plumes in the tropopause region and implications for ozone, *Science*, *282*, 1305-1309, 1998.

Chameides, W. L. and J. C. G. Walker, A photochemical theory of tropospheric ozone, *J. Geophys. Res.*, *78*, 8751-8760, 1973.

Chameides, W. L., D. D. Davis, J. Bradshaw, M. Rodgers, S. Sandholm, and D. B. Bai, An estimate of the NO_x production rate in electrified clouds based on NO observations from the GTE/CITE 1 fall 1983 field operation, *J. Geophys. Res.*, *92*, 2153-2156, 1987.

Chatfield, R. B., Anomalous HNO_3/NO_x ratio of remote tropospheric air: Conversion of nitric acid to formic acid and NO_x?, *Geophys. Res. Lett.*, *21*, 2705-2708, 1994.

Cohan, D. S., M G. Schultz, D. J. Jacob, B. G. Heikes, and D. R. Blake, Convective injection and photochemical decay of peroxides in the tropical upper troposphere: Methyl iodide as a tracer of marine convection, *J. Geophys. Res.*, *104*, 5717-5724, 1999.

Crawford, J., et al., Implications of large scale shifts in tropospheric NO_x levels in the remote tropical Pacific, *J. Geophys. Res.*, *102*, 28,447-28,468, 1997.

Crawford, J., D. Davis, J. Olson, G Chen, S. Liu, G. Gregory, J. Barrick, G. Sachse, S. Sandholm, B. Heikes, H. Singh, and D. Blake, Assessment of upper tropospheric HO_x sources over the tropical Pacific based on NASA/GTE PEM data: Net effect on HO_x and other photochemical parameters, *J. Geophys. Res.*, *104*, 16,255-16,273, 1999.

Crutzen, P., A discussion of the chemistry of some minor constituents in the stratosphere and troposphere, *Pure Appl. Geophys.*, *106-108*, 1385-1399, 1973.

Cummins, K. L., M. J. Murphy, E. A. Bardo, W. L. Hiscox, R. B. Pyle, and A. E. Pifer, A combined TOA/MDF technology upgrade of the U.S. National Lightning Detection Network, *J. Geophys. Res.*, *103*, 9035-9044, 1998.

Davis, D. D., et al., Assessment of ozone photochemistry in the western North Pacific as inferred from PEM-West A observations during the fall of 1991, *J. Geophys. Res.*, *101*, 2111-2134, 1996.

Davis, D., M. Buhr, J. Nowak, G. Chen, R. Mauldin, F. Eisele, and D. Tanner, Unexpected high levels of NO at South Pole: Observations and chemical consequences, *EOS Trans. AGU*, 80(17), Fall Meet. Suppl., F190, 1999.

Dransfield, T. J., K. K. Perkins, N. M. Donahue, J. G. Anderson, M. M. Sprengnether, and K. L. Demerjian, Temperature and pressure dependent kinetics of the gas-phase reaction of the hydroxyl radical with nitrogen dioxide, *Geophys. Res. Lett.*, *26*, 687-690, 1999.

Fan, S.-M., D. J. Jacob, D. L. Mauzerall, J. D. Bradshaw, S. T. Sandholm, D. R. Blake, H. B. Singh, R. W. Talbot, G L. Gregory, and G. W. Sachse, Origin of tropospheric NO_x over subarctic eastern Canada in summer, *J. Geophys. Res.*, *99*, 16,867-16,877, 1994.

Feigl, C., H. Schlager, H. Ziereis, J. Curtius, F. Arnold, and C. Schiller, Observation of NO_y uptake by particles in the Arctic tropopause region at low temperatures, *Geophys. Res. Lett.*, *26*, 2215-2218, 1999.

Flatøy, F., and Ø. Hov, NO_x from lightning and the calculated chemical composition of the free troposphere, *J. Geophys. Res.*, *102*, 21,373-21,381, 1997.

Fuelberg, H. E., J. R. Hannan, P. F. J. van Velthoven, E. V. Browell, G. B. Bieberbach Jr., R. D. Knabb, K. E. Pickering, and H. B. Selkirk, A meteorological overview of the Subsonic Assessment Ozone and Nitrogen Oxide Experiment (SONEX) period, *J. Geophys. Res.*, *105*, 3633-3652, 2000.

Hameed, S., J. P. Pinto, and R. W. Stewart, Sensitivity of the predicted CO-OH-CH_4 perturbation to tropospheric NO_x concentrations, *J. Geophys. Res.*, *84*, 763-768, 1979.

Hannan, J. R., et al., Atmospheric chemical transport based on high-resolution model-derived winds: A case study, *J. Geophys. Res.*, *105*, 3807-3820, 2000.

Hauglustaine, D. A., B. A. Ridley, S. Solomon, P. G. Hess, and S. Madronich, HNO_3/NO_x ratio in the remote troposphere during MLOPEX 2: Evidence for nitric acid reduction on carbonaceous aerosols, *Geophys. Res. Lett.*, *23*, 2609-2612, 1996.

Höller, H., U. Finke, H. Huntreiser, M. Hagen, and C. Feigl, Lightning-produced NO_x (LINOX): Experimental design and case study results, *J. Geophys. Res.*, *104*, 13,911-13,922, 1999.

Honrath, R. E., M. C. Peterson, S. Guo, J. E. Dibb, P. B. Shepson, and B. Campbell, Evidence of NO_x production within or upon ice particles in the Greenland snowpack, *Geophys. Res. Lett.*, *26*, 695-698, 1999.

Houweling, S., F. Dentener, and J. Lelieveld, The impact of nonmethane hydrocarbon compounds on tropospheric photochemistry, *J. Geophys. Res.*, *103*, 10,673-10,696, 1998.

Huntreiser, H., H. Schlager, C. Feigl, and H. Höller, Transport and production of NO_x in electrified thunderstorms. Survey of previous studies and new observations at midlatitudes, *J. Geophys. Res.*, *103*, 28,247-28,264, 1998.

Idone, V. P , D. A. Davis, P. K. Moore, Y. Wang, R. W. Henderson, M. Ries, and P. F. Jamason, Performance evaluation of the U S. National Lightning Detection Network in eastern New York, 1, Detection efficiency, *J. Geophys. Res.*, *103*, 9045-9055, 1998a.

Idone, V. P., D. A. Davis, P. K. Moore, Y. Wang, R. W. Henderson, M. Ries, and P. F. Jamason, Performance evaluation of the U.S. National Lightning Detection Network in eastern New York, 2, Location accuracy, *J. Geophys. Res.*, *103*, 9057-9069, 1998b.

Iraci, L T., and M A. Tolbert, Heterogeneous interaction of formaldehyde with cold sulfuric acid. Implications for the upper troposphere and lower stratosphere, *J. Geophys. Res.*, *102*, 16,099-16,107, 1997

Jacob, D. J., et al., Origin of ozone and NO_x in the tropical troposphere: A photochemical analysis of aircraft observations over the South Atlantic basin, *J. Geophys. Res.*, *101*, 24,235-24,250, 1996.

Jaeglé, L., et al., Observed OH and HO_2 in the upper troposphere suggest a major source from convective injection of peroxides, *Geophys. Res. Lett.*, *24*, 3181-3184, 1997.

Jeker, D. P., L. Pfister, A. M. Thompson, D. Brunner, D. J. Boccippio, K. E. Pickering, H. Wernli, Y. Kondo, and J. Staehelin, Measurements of nitrogen oxides at the tropopause: Attribution to convection and correlation with lightning, *J. Geophys. Res.*, *105*, 3679-3700, 2000.

Jones, A. E., R. Weller, E. W. Wolff, and H.-W. Jacobi, Speciation and rate of photochemical NO and NO_2 production in Antarctic snow, *Geophys. Res. Lett.*, *27*, 345-348, 2000.

Lary, D. J., A. M. Lee, R. Toumi, M. J. Newchurch, M. Pirre, and J. B. Renard, Carbon aerosols and atmospheric photochemistry, *J. Geophys. Res.*, *102*, 3671-3682, 1997.

Lawrence, M. G., W. L. Chameides, P. S. Kasibhatla, H. Levy II, and W. Moxim, Lightning and atmospheric chemistry: The rate of atmospheric NO production, in *Handbook of Atmospheric Electrodynamics*, vol. 1, edited by H. Volland, pp. 189-202, CRC Press, Boca Raton, Fla., 1995.

Lee, D. S., et al., Estimations of global NO_x emissions and their uncertainties, *Atmos. Environ.*, *31*, 1735-1749, 1997.

Levy, H., II, W. J. Moxim, and P. S. Kasibhatla, A global three-dimensional time-dependent lightning source of tropospheric NO_x, *J. Geophys. Res.*, *101*, 22,911-22,922, 1996.

Liaw, Y. P., D. L. Sisterson, and N. L. Miller, Comparison of field, laboratory, and theoretical estimates of global nitrogen fixation by lightning, *J. Geophys. Res.*, *95*, 22,489-22,494, 1990.

Liu, S. C., Possible effects on tropospheric O_3 and OH due to NO emissions, *Geophys. Res. Lett.*, *4*, 325-328, 1977.

Liu, S. C., M. Trainer, F. C. Fehsenfeld, D. D. Parrish, E. J. Williams, D. W. Fahey, G. Hubler, and P. C. Murphy, Ozone production in the rural troposphere and the implications for regional and global ozone distributions, *J. Geophys. Res.*, *92*, 10,463-10,482, 1987.

Liu, S. C., et al., A study of the photochemistry and ozone budget during the Mauna Loa Observatory Photochemistry Experiment, *J. Geophys. Res.*, *97*, 10,463-10,471, 1992.

Liu, S. C., et al., Sources of reactive nitrogen in the upper troposphere during SONEX, *Geophys. Res. Lett.*, *26*, 2441-2444, 1999.

Meijer, E. W., P. F. J. van Velthoven, W. M. F. Wauben, J. P. Beck, and G. J. M. Velders, The effects of the conversion of nitrogen oxides in aircraft exhaust plumes in global models, *Geophys. Res. Lett.*, *24*, 3013-3016, 1997.

Meilinger, S. K., et al., HNO_3 partitioning in cirrus clouds, *Geophys. Res. Lett.*, *26*, 2207-2210, 1999.

O'Sullivan, D. W., B. G. Heikes, M. Lee, W. Chang, G. L. Gregory, D. R. Blake, and G. W. Sachse, Distribution of hydrogen peroxide and methylhydroperoxide over the Pacific and South Atlantic Oceans, *J. Geophys. Res.*, *104*, 5635-5646, 1999.

Penner, J. E., D. J. Bergmann, J. W. Walton, D. Kinnison, M. J. Prather, D. Rotman, C. Price, K. E. Pickering, and S. L. Baughcum, An evaluation of upper troposphere NO_x with two models, *J. Geophys. Res.*, *103*, 22,097-22,113, 1998.

Pickering, K. E., Y Wang, W.-K. Tao, C. Price, and J.-F. Müller, Vertical distributions of lightning NO_x for use in regional and global chemical transport models, *J. Geophys. Res.*, *103*, 31,203-31,216, 1998.

Price, C. and D. Rind, A simple parameterization for calculating global lighting distributions, *J. Geophys. Res.*, *97*, 9919-9933, 1992.

Price, C., J. Penner, and M. Prather, NO_x from lightning, 1, Global distribution based on lightning physics, *J. Geophys. Res.*, *102*, 5929-5941, 1997.

Proctor, D. E., Regions where lightning flashes began, *J. Geophys. Res.*, *96*, 5099-5112, 1991.

Ridley, B. A., J. E. Dye, J. G. Walega, J. Zheng, F. E. Grahek, and W.

Rison, On the production of active nitrogen by thunderstorms over New Mexico, *J. Geophys. Res.*, *101*, 20,985-21,005, 1996.

Schultz, M. G , D. J. Jacob, J. D. Bradshaw, S. T. Sandholm, J. E. Dibb, R. W. Talbot, and H. B. Singh, Chemical NO_x budget in the upper troposphere over the tropical South Pacific, *J. Geophys. Res.*, *105*, 6669-6679, 2000.

Sillman, S., J. A. Logan, and S. C. Wofsy, Regional scale model for ozone in the United States with subgrid representation of urban and power plant plumes, *J. Geophys. Res.*, *95*, 5731-5748, 1990.

Singh, H. B., A. Thompson, and H. Schlager, SONEX airborne mission and coordinated POLINAT-2 activity: Overview and accomplishments, *Geophys. Res. Lett.*, *26*, 3053-3056, 1999.

Stockwell, D. Z., C. Giannakopoulos, P.-H. Plantevin, G. D. Carver, M. P. Chipperfield, K. S. Law, J. A. Pyle, D. E. Shallcross, and K -Y. Wang, Modelling NO_x from lightning and its impact on global chemical fields, *Atmos. Environ.*, 33, 4477-4493, 1999

Tabazadeh, A., O. B. Toon, and E. J. Jensen, A surface chemistry model for nonreactive trace gas adsorption on ice: Implications for nitric acid scavenging by cirrus, *Geophys. Res. Lett.*, *26*, 2211-2214, 1999.

Thompson, A. M., L C. Sparling, Y. Kondo, B. E. Anderson, G. L. Gregory, and G. W. Sachse, Perspectives on NO, NO_y and fine aerosol sources and variability during SONEX, *Geophys. Res. Lett.*, *26*, 3073-3076, 1999

Wang, Y., D. J. Jacob, and J A. Logan, Global simulation of tropospheric O_3-NO_x-hydrocarbon chemistry, 1, Model formulation, *J. Geophys Res.*, *103*, 10,713-10,725, 1998.

Wang, Y., S. C. Liu, B. E. Anderson, Y. Kondo, G. L. Gregory, G W. Sachse, S. A. Vay, D R. Blake, H. B. Singh, and A. M. Thompson, Evidence of convection as a major source of condensation nuclei in the northern midlatitude upper troposphere, *Geophys. Res. Lett.*, *27*, 369-372, 2000.

Weinheimer, A. J., T. L. Campos, J. G. Walega, F. E. Grahek, B. A. Ridley, and E. J. Jensen, Uptake of NO_y on wave-cloud ice particles, *Geophys. Res. Lett.*, *25*, 1725-1728, 1998.

Winterrath, T., T. P. Kurosu, A. Richter, and J. P. Burrows, Enhanced O_3 and NO_2 in thunderstorm clouds: Convection or production?, *Geophys. Res. Lett.*, *26*, 1291-1294, 1999.

Zondlo, M. A., S. B. Barone, and M. A. Tolbert, Uptake of HNO_3 on ice under upper tropospheric conditions, *Geophys. Res. Lett.*, *24*, 1391-1394, 1997.

B. Anderson, J. Crawford, G. Gregory, J. Olson, and G. Sachse, NASA Langley Research Center, 21 Langley Boulevard, Hampton, VA 23681-0001. (j.h.crawford@larc.nasa.gov)

D. Blake, Department of Chemistry, University of California, Irvine, Irvine, CA 92717

G. Chen, D. Davis, and S. Liu, School of Earth and Atmospheric Sciences, Georgia Institute of Technology, Atlanta, GA 30332.

H. Fuelberg and J. Hannan, Department of Meteorology, Florida State University, Tallahassee, FL 32306.

B. Heikes and J. Snow, Center for Atmospheric Chemistry Studies, University of Rhode Island, Narragansett, RI 02882.

Y. Kondo, Solar Terrestrial Environment Laboratory, Nagoya University, Toyokawa, Aichi, Japan.

H Singh, NASA Ames Research Center, Moffett Field, CA 94035.

R Talbot, Institute for the Study of Earth, Oceans, and Space, University of New Hampshire, Durham, NH 03820.

A. Viggiano, Air Force Research Laboratory, Hanscom Air Force Base, MA 01731

(Received January 19, 2000; revised March 14, 2000,
accepted March 15, 2000)